CrossMark

Mission Considerations for Transfers to a Distant Retrograde Orbit

Chelsea M. Welch[1,2] · **Jeffrey S. Parker**[2] ·
Caley Buxton[3]

Abstract This paper discusses the applications of Distant Retrograde Orbits (DROs) about the Moon in support of advanced concepts such as NASA's Asteroid Redirect Mission. It studies how to build a direct transfer from a low Earth orbit to a DRO, paying attention to the navigation challenges of each transfer option. The characteristics of planar DROs in the Earth-Moon system are examined. The paper focuses on a DRO that is in a 2:1 resonance with the lunar synodic period. Trade studies illustrate the relationships between the transfer trajectory duration, required launch energy, and DRO orbit insertion Δv cost. In addition, powered lunar flyby transfers are explored to determine potential cost savings in Δv. These investigations are conducted in both the Circular Restricted Three-Body system and in a high-fidelity model of the solar system.

✉ Caley Buxton
  caley.j.buxton@lmco.com

  Chelsea M. Welch
  chelsea.m.welch@lmco.com

  Jeffrey S. Parker
  parkerjs@colorado.edu

1 Lockheed Martin Civil Space Advanced Programs,
   Mail Stop S8110, P.O. Box 179, Denver, CO 80201, USA

2 Department of Aerospace Engineering Sciences, Colorado Center for Astrodynamics Research,
   431 UCB, University of Colorado, Boulder, CO 80309-0431, USA

3 Lockheed Martin Civil Space Advanced Programs,
   Mail Stop H3005, P.O. Box 179, Denver, CO 80201, USA

Introduction

NASA is considering placing an asteroid into a Distant Retrograde Orbit (DRO) about the Moon as part of its Asteroid Redirect Mission (ARM) concept [1, 2]. DROs about the Moon are prime candidates for the ARM concept for several reasons, including their long-term stability and the low fuel cost needed for insertion. An asteroid placed into a properly designed DRO may remain there for centuries [1–3]. Without using deterministic maneuvers, it is possible to enter a DRO from outside the Earth's sphere of influence [4]. These results highlight the benefits of the DRO as a storage orbit for the asteroid. The purpose of the current study is to evaluate the costs and benefits of different orbit transfer strategies for a crewed vehicle to depart a low-Earth orbit and rendezvous with an asteroid or other object already placed in the DRO. The results drive the requirements of the crewed vehicle, and may drive the design trade space of the asteroid's storage orbit.

Two significant drivers for a crewed mission to a DRO are flight time and fuel consumption. This paper considers two distinct strategies to transfer the crewed vehicle from the Earth to the DRO: a *direct transfer*, where the spacecraft departs the Earth, travels to the DRO, and inserts into the DRO, and a *powered lunar flyby* (PLF) transfer, where the spacecraft departs the Earth, travels to a point near the Moon, executes a maneuver to leverage the lunar flyby, and then proceeds to travel to the DRO. The direct transfer is operationally simpler and often requires less flight time. The PLF transfer may be designed to use less fuel. These options are fully characterized here, with special consideration given to the navigation challenges of each transfer strategy.

The transfers studied here are first examined in the Circular Restricted Three-Body Problem (CRTBP)[5, 6] in order to evaluate trends that exist in every month, and then examined in a high-fidelity model of the solar system.

Background

Lunar *Distant Retrograde Orbits* revolve about the Moon in a clockwise fashion when viewed from above in the Earth-Moon rotating coordinate frame. Many people contributed to the discovery of DROs, including [7–9], and Broucke[10]. DROs were first constructed in the planar CRTBP, i.e., a simplified model where a spacecraft is restricted to travel in the orbital plane of two massive bodies, such as the Earth and the Moon [5, 6]. The CRTBP is a powerful system to use as a model since it captures the main features of the trajectories without exposing them to variations from realistic perturbations, such as the Moon's non-circular orbit and the gravitational influence of the Sun and other planets. Planar DROs in the Earth-Moon CRTBP may be designed to be perfectly periodic, such that they repeat after some time when viewed in the rotating frame. Realistic DROs are never perfectly periodic, given the varying perturbations in the Z-axis, among other non-periodic perturbations. Near-planar DROs have been found to be more stable than three-dimensional DROs [11]. Thus, near-planar orbits are considered here. The transfers constructed in the CRTBP

are entirely planar while the transfers constructed in the high-fidelity model of the solar system include small-amplitude Z-axis motion.

DROs with orbit periods that are near a 2:1 resonance with the lunar synodic period of 29.53 days are useful because they provide repeating geometry between the Earth, Sun, and Moon, supporting missions that involve assets on the lunar surface that require proper lighting. A new mission opportunity occurs twice every synodic month, which is advantageous in the event of a missed launch.

Figure 1 shows four different DROs with various lunar resonances. The 2:1 resonant orbit (the second largest in Fig. 1) has a closest approach to the Moon of approximately 70,000 km and a maximum distance of approximately 90,000 km. The insertion angle, τ(tau), of the DRO is shown on the plot for reference, where τ is defined to advance in a clockwise fashion at a constant rate in time, mimicking the mean anomaly of Keplerian orbits [6].

Methodology

This study uses three different approaches to examine the trade space of trajectories that may be used to transfer a spacecraft from a low Earth orbit (LEO) to a DRO. First, *direct transfers* are explored in the planar CRTBP. These transfers perform two deterministic maneuvers: one to depart LEO and one to insert into the DRO. Lunar flybys may be included, but are not targeted specifically. Second, *powered lunar flyby* (PLF) transfers are constructed in the planar CRTBP, where a targeted lunar flyby is included in the design and the spacecraft executes a maneuver near the periapse of the flyby. Third, PLF transfers are constructed in the high-fidelity ephemeris system in order to identify variations that exist in the real solar system. This model includes realistic non-coplanar orbits and perturbations and also introduces three-dimensional aspects of the transfer problem, such as departing from a 28.5° inclined parking orbit. Transfers are also constructed at different points in the Moon's orbit
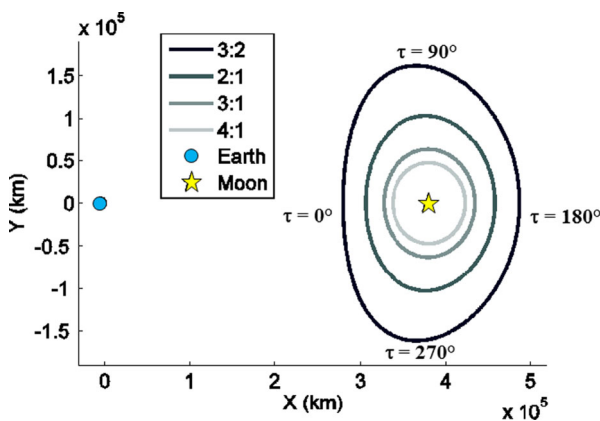

Fig. 1 Distant Retrograde Orbits with Lunar Resonances in the Earth-Moon Rotating Frame

about the Earth. The high-fidelity transfers demonstrate trends that are very similar to those observed in the planar CRTBP, giving credence to the CRTBP simplifications. The methodology used for the planar CRTBP trajectories is given below. Further details for the methodology used in the high-fidelity simulations will be discussed later.

The transfers constructed in the CRTBP leave Earth from a 300-km parking orbit. A Δv burn that is tangential to the Earth parking orbit is used to enter the transfer orbit and a second burn in the X and Y directions at the end of the transfer is used to insert into the DRO, though not necessarily tangential to it. The direct transfers are designed to take either 5, 7, or 9 days to reach the DRO. The PLF transfers take variable durations and are constrained to be less than 13 days. This 13-day constraint is arbitrary but forces the solutions to remain within a short-duration class, compatible with approximate roundtrip duration of 30 days. The PLF trajectories also perform a burn in the X and Y directions near lunar closest approach before the DRO insertion burn. This closest-approach burn is not necessarily tangential to the incoming trajectory and is not constrained to be located at perilune, but it must occur at an altitude of 100 km or more.

Direct transfers have been found for all τ insertion angles. As will be seen later, there are two options for direct transfer trajectories for certain insertion angles: flybys of the near side or far side of the Moon. Both options have advantages and disadvantages, which will be seen in the Results section of the paper. PLF transfers have been found for specific τ insertion angles in the CRTBP. These will be compared with direct transfers to the same locations, as well as to high-fidelity PLFs generated with the full planetary ephemeris.

Direct transfers to DROs are constructed using MATLAB. A Runge-Kutta 7/8 integrator is used to numerically integrate the trajectory in the CRTBP [12]. MATLAB's built-in constrained non-linear optimizer *fmincon* optimizes the direct transfers by minimizing the Δv required for insertion into the DRO. This optimization utilizes four control variables: the angular location of the LEO-departure maneuver in the parking orbit (ν_{Earth}), the tangential Δv from the Earth parking orbit onto the transfer orbit (Δv_{Earth}), and the $X-$ and $Y-$components of the DRO-insertion Δv ($\Delta v_{X,\text{DRO}}$ and $\Delta v_{Y,\text{DRO}}$). Figure 2 illustrates a schematic of the optimization algorithm setup for direct transfers.

To begin, the state of the spacecraft at Earth is defined based on the initial guess for the control variables Δv_{Earth} and ν_{Earth}. The state of the spacecraft on the DRO is defined based on the particular τ insertion angle being targeted and the initial guess for the control variables $\Delta v_{X,\text{DRO}}$ and $\Delta v_{Y,\text{DRO}}$. The algorithm proceeds by propagating the state of the spacecraft at Earth departure forward for half the desired transfer duration (the blue segment in Fig. 2) while the state at the DRO is propagated backward half the transfer duration (the red segment in Fig. 2). The optimizer is constrained to find a solution such that the final positions and velocities of the two trajectories match at the transfer's mid-point, i.e., $\Delta X_{\text{mid}} = \Delta Y_{\text{mid}} = \Delta V_{X,\text{mid}} = \Delta V_{Y,\text{mid}} = 0$ (see Fig. 2), to within a small tolerance. When the matching point is far from both the Earth and the Moon, the dynamics are smoother and more linear. This aids in the convergence of the algorithm, hence the reason half the transfer duration is utilized in both propagation segments.
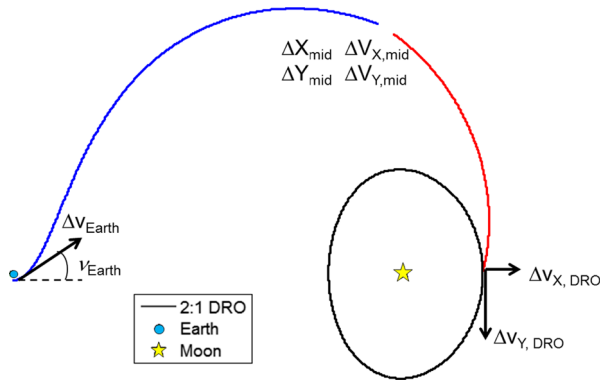
Fig. 2 Schematic of Direct-Transfer Optimization Setup

In order to find a continuous trajectory, the difference in position at the middle in both the X and Y directions is constrained to be less than 1 km while the difference in velocity is constrained to be less than 1 cm/sec. All control and constraint variables, including the objective function, are further normalized by some fixed value at the beginning of the simulation in order to keep each variable between approximately ± 1. This method ensures that the optimizer can vary each parameter equivalently during the optimization, allowing for even better stability and convergence of the algorithm.

To construct the PLF trajectories, a similar algorithm, but using four propagation segments instead of two, has been utilized. The initial state at the Earth and DRO insertion are defined exactly the same as before. Now, however, there are two additional states, and the positions of both are defined at the location of the PLF near the Moon. Segment 1 propagates forward from Earth departure and meets Segment 2, which is propagated backward from the PLF. Segment 3 propagates forward from the PLF and joins Segment 4, which is propagated backward from the DRO insertion. The position of Segments 2 and 3 at the PLF are constrained to be equal, but the PLF Δv arises from a difference in velocity at this point. The positions and velocities where Segments 1 and 2 meet and where Segments 3 and 4 meet are constrained to be equal, within tolerances of 1 km and 1 cm/s, respectively. Figure 3 illustrates this setup.

The PLF optimization requires the same control variables as the direct-transfer optimization plus an additional eight control variables. These include the incoming and outgoing velocity at the PLF in the X and Y directions ($v_{X,Y,in,PLF}$ and $v_{X,Y,out,PLF}$), the angular location of the PLF with respect to the Earth-Moon line in the rotating frame (defined similarly to v_{Earth}), the altitude of closest approach at the PLF, the time between Earth departure and the PLF, and the time between the PLF and DRO insertion. Breaking the total transfer duration up into two variable segments allows the optimizer to converge to the best overall transfer duration and prevents over-constraining of the problem. In addition, while Segments 1 and 2 are both propagated one half of the time between Earth departure and the PLF, Segment 3 is propagated three quarters of the time between the PLF and DRO insertion,
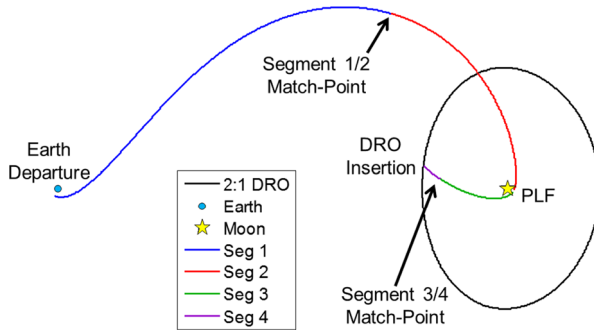
Fig. 3 Schematic of PLF Optimization Setup

while Segment 4 is propagated one quarter of that time. This is to place the match-point as far from the Moon as possible, which again allows for smoother dynamics and better convergence. Similar normalization occurs for the PLF control and constraint variables as was utilized in the direct-transfer algorithm. The quantity the optimizer minimizes is the sum of the PLF Δv and the DRO insertion Δv, shown in Eq. 1.

$$\Delta v = \sqrt{\Delta v_{X,DRO}^2 + \Delta v_{Y,DRO}^2} + \sqrt{(v_{X,out,PLF} - v_{X,in,PLF})^2 + (v_{Y,out,PLF} - v_{Y,in,PLF})^2} \quad (1)$$

Direct Transfer Results

This section presents a summary of the optimized direct transfers to a 2:1 DRO for 5-, 7-, and 9-day transfer durations, focusing on required Δv insertion cost, launch C_3 energy, and radius of closest approach to the Moon. Navigation considerations are also addressed. Later, the direct transfer results will be compared to the PLF results to understand how PLFs can provide cost savings in terms of overall mission Δv.

Table 1 summarizes the average LEO-departure Δv and the maximum and minimum values over all insertion angles, as well as the launch energy parameter C_3, for all three transfer-duration cases. Generally, longer transfer durations are less efficient, travel further from Earth (Fig. 4 through Fig. 6), and require more Δv for Earth departure. A longer transfer duration and corresponding larger Δv also requires a larger C_3, as expected. It should be noted that since the variation in required Earth-departure Δv over all transfer durations and all insertion angles is only 39 m/s, and since the upper stage of a launch vehicle likely performs this burn, performance assessments of each transfer do not include this quantity and thus it does not appear in the optimization Δv objective function.

Table 1 Average Δ v and Variation over All Insertion Angles Required for Transfer from a 300-km Earth Parking Orbit to Direct-Transfer Trajectory (Launch Energy C_3 is Included for Reference)

Transfer Duration (days)	Avg. Δ v $_{Earth}$ (km/s)	Min Δv_{Earth} (km/s)	Max Δv_{Earth} (km/s)	Avg. C_3 (km^2/s^2)	Min C_3 (km^2/s^2)	Max C_3 (km^2/s^2)
5	3.1082	3.0886	3.1277	−2.0039	−2.4271	−1.5807
7	3.1133	3.1030	3.1236	−1.8930	−2.1173	−1.6687
9	3.1204	3.1140	3.1268	−1.7390	−1.8784	−1.5996

Direct Transfers for 5-, 7-, and 9-Day Durations

Figure 4 shows optimized direct transfers to the 2:1 DRO for a 5-day transfer. Trajectories are achieved for all τ insertion angles attempted. The single dotted line on the figure represents the radius of the Moon's orbit about the Earth, provided for perspective. Most of the 5-day trajectories remain within one Earth-Moon radius during the transfer unless the insertion point is located outside this distance, such as occurs with the far-side insertion transfers.

In addition, for insertion angles between 170° and 360°, there are two options for transfer trajectories: those that pass on the near side of the Moon and those that pass
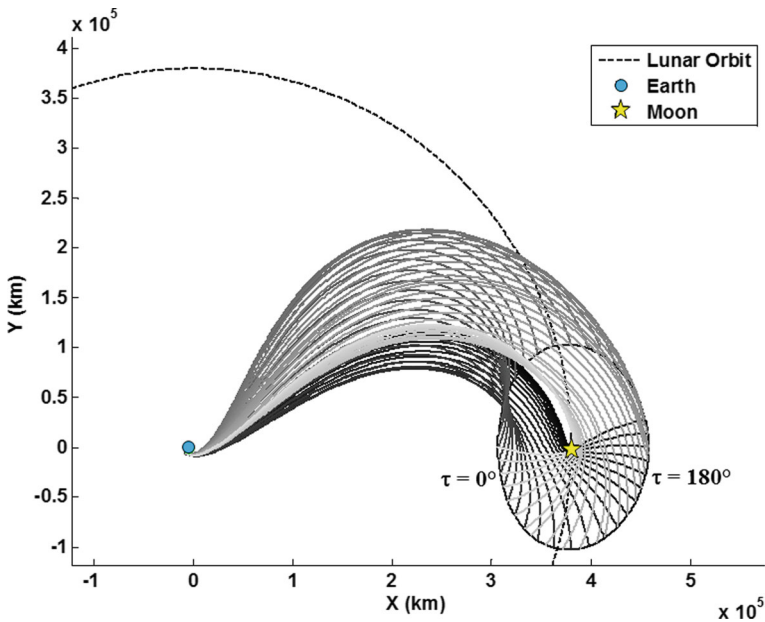
Fig. 4 Direct 5-Day Transfers to a 2:1 DRO for Each τ Insertion Angle

on the far side. This investigation imposes a minimum lunar flyby altitude of 100 km. Both families of transfers extend as far in their insertion angles as possible until hitting that constraint (about 360° for the far-side transfers and 170° for the near-side ones).

It should be noted that the transfers often appear to require a very large maneuver to insert into the DRO. For instance, the darker trajectories that arrive near $\tau = 0°$ appear to reverse direction entirely upon arrival at the DRO. This direction reversal is a feature of illustrating the transfers in a rotating coordinate frame. The transfer trajectory arrives at the DRO such that the vehicle's mean motion is smaller than the Moon's, and the DRO's mean motion is greater than the Moon's. Therefore, the trajectory must reverse direction in the rotating frame. In the inertial frame, each of these transfers resembles an intuitive Hohmann-like transfer.

Figure 5 shows optimized direct transfers to the 2:1 DRO for a 7-day transfer. The general features of this trade space resemble those shown in Fig. 4. Two types of transfers can also be seen here between insertion angles of approximately 180° and 45°, both ending at 100-km lunar flybys over the near and far sides of the Moon. In addition, due to the longer transfer duration, trajectories travel outside the Earth-Moon distance before reaching the DRO more often than for 5-day transfers.

Figure 6 shows optimized direct transfers to the 2:1 DRO for a 9-day transfer. Again, two types of transfers occur, this time between insertion angles of
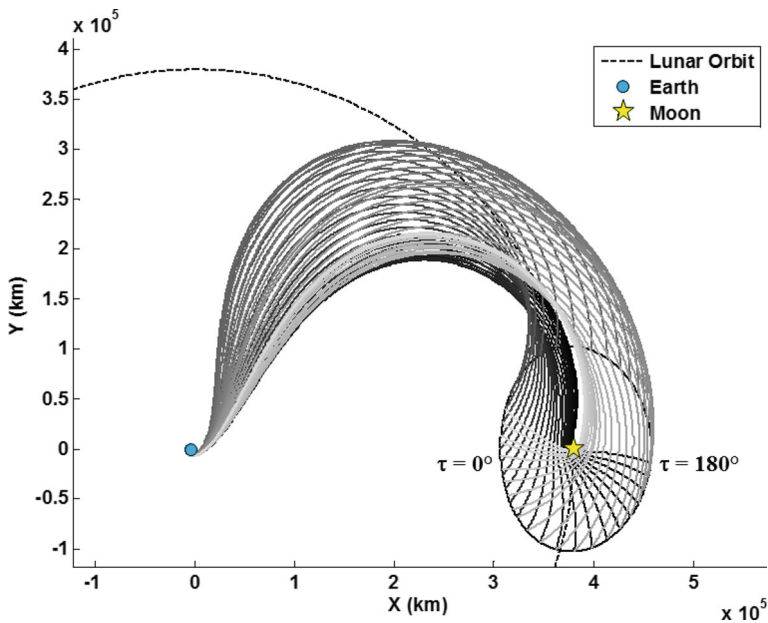

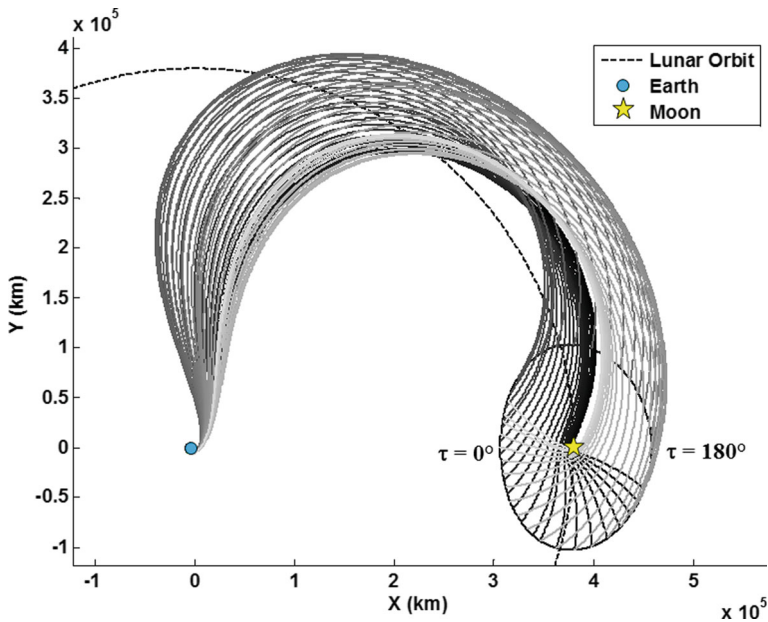**Fig. 5** Direct 7-Day Transfers to a 2:1 DRO for Each τ Insertion Angle

200° and 25°. For the 9-day case, all transfers pass outside the Earth-Moon distance due to the longer transfer duration. As mentioned before, the higher-apogee radii require somewhat more Δv for Earth departure than for the shorter transfers.
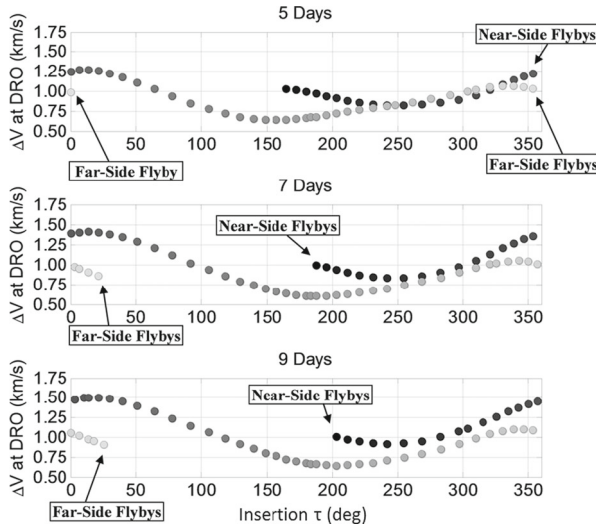
Required ΔV for DRO Insertion

Figure 7 shows the required DRO insertion Δv for the 5-, 7-, and 9-day transfers. The darkest circles represent the near-side lunar flybys while the lightest circles represent the far-side lunar flybys, matching the shading in Figs. 4, 5, and 6.

For the 7- and 9-day transfers, in order to access the DRO between insertion angles of approximately 200° to 25°, the lighter-colored far-side lunar flybys are much more cost effective than the ones that occur on the near-side. The cost savings may be as high as 0.5 km/s, depending on the insertion angle. For the 5-day transfer, the far-side flybys are more efficient in this region except for the insertion angles of approximately 250° to 320° where the near-side flybys allow for slightly less Δv.

Table 2 shows the minimum Δv for each transfer duration case and its corresponding insertion angle. For each case, the trajectory has its minimum Δv when it inserts into the DRO on the far side of the Moon.

Fig. 6 Direct 9-Day Transfers to a 2:1 DRO for Each τ Insertion Angle

Fig. 7 Required DRO Insertion Δv for 5-, 7-, and 9-Day Transfers

## Parameter Comparison for Different Transfer Durations

Figure 8 shows a comparison between the required Δv for DRO insertion, C_3 launch energy, and lunar radius of closest approach for all three transfer durations. For clarity, in these figures the two options for transfer trajectories are shown by the repeating insertion angle on the horizontal axis, as opposed to the overlap seen in the previous figure. The far left side of these plots shows the near-side lunar flybys while the right side shows the far-side flybys.

There is a tradeoff between the required launch C_3 energy and the DRO insertion Δv. Generally, less Δv at the DRO insertion requires a higher C_3. This is especially true for the 5-day transfers, which see the largest change in required launch energy depending on the DRO insertion angle. However, the equivalent Δv variation caused by the variation in launch C_3 is relatively small, which was seen to be 39 m/s in Table 1, compared to hundreds of m/s in the DRO insertion range.

It can also be seen that the 9-day transfers require the most Δv and the 5-day transfers require the least across all insertion angles except for the trajectories between 180° and 315°, which pass by the far side of the Moon (right half of the figure). In this region, the 5-day trajectories require the most Δv. Here, the 7-day transfers become more efficient and are similar to the 9-day transfer performance.

Table 2 Minimum Δv for Each Transfer Duration and Corresponding Insertion Angle

| Transfer Duration (days)	5	7	9
Minimum Δv (km/s)	0.639	0.608	0.648
Insertion Angle (deg)	157	188	203
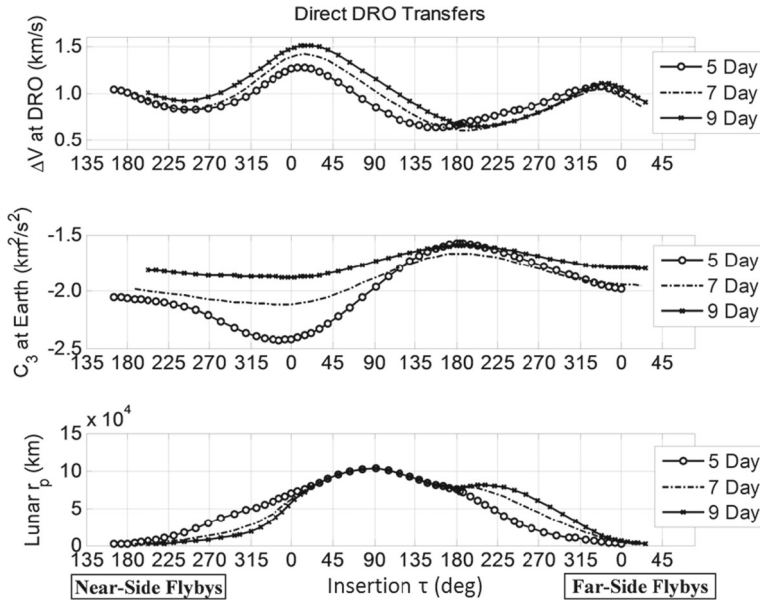
Fig. 8 Comparison of Required DRO Insertion Δv, C_3 Launch Energy, and Lunar Radius of Closest Approach for 5-, 7-, and 9-Day Transfers

Challenges for Navigation

Spacecraft operators have acquired a great deal of experience navigating spacecraft to the Moon on trajectories shorter than 9 days in duration. Longer durations provide more time for orbit determination and maneuver planning, but even 5 days is reasonable for a DRO transfer. The more concerning navigation challenge is how close these transfers may get to the Moon. Transfers that include a low-altitude lunar flyby require careful navigation and often include at least one statistical targeting maneuver. For the purpose of describing the trade space, a transfer is defined to include a lunar flyby if a spacecraft's lunar radius ever drops below 20,000 km (perilune altitude below 18,262 km). For these cases, it is important to ensure sufficient time, ideally at least one day, between the lunar flyby event and the DRO insertion event in order to allow for navigation planning.

Figure 9 shows the radius of closest approach for transfers that pass by the Moon at a radius of 20,000 km or less. Solid black points indicate less than one day between closest approach and DRO insertion while white points indicate more than one day. Several of the flyby trajectories with radii smaller than 20,000 km do not provide at least one day between lunar closest approach and DRO insertion for proper navigation planning, so it may be necessary to avoid these flyby trajectories and use alternatives that pass by at a higher altitude but on the other side of the Moon. However, the time between these two events is never less than 0.75 days, which may be sufficient for navigation.
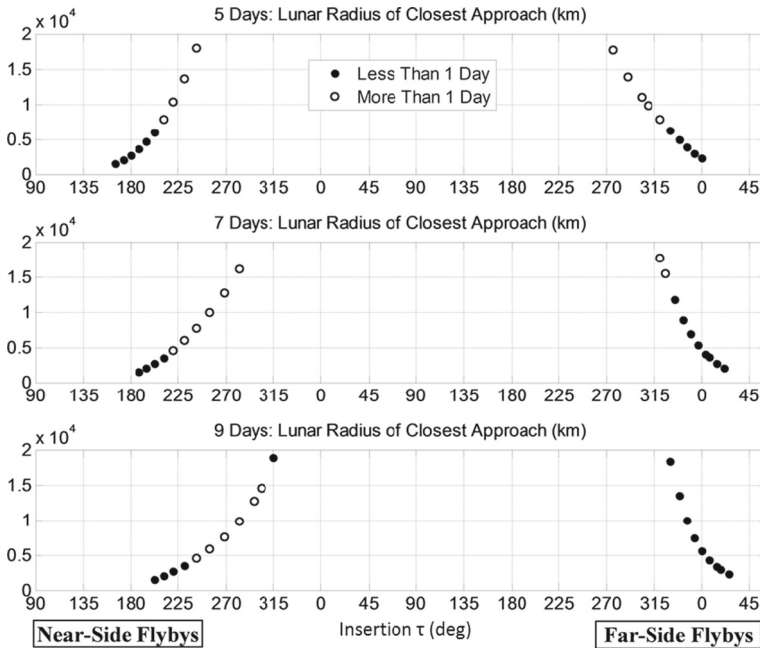
Fig. 9 Lunar Radius of Closest Approach with Indication when Time Between Closest Approach and DRO Insertion is Less Than One Day for Transfers Passing the Moon at 20,000 km or Less

Powered Lunar Flyby Results

Several of the direct transfers pass very near the Moon, indicating that a powered lunar flyby may save fuel since energy-changing maneuvers performed close to the Moon are more efficient, via the Oberth Effect. Therefore, the following sections describe the construction and optimization of several PLF trajectories to the 2:1 DRO and compare them to the direct transfers previously described. The first investigation remains in the planar CRTBP. The final investigation examines PLF transfers within a realistic model of the solar system.

Far-Side Powered Lunar Flybys

PLFs that pass by the far side of the Moon have been found between insertion angles of -30° and 210° (Fig. 10). Unlike for the direct transfers, which are unable to enter into an insertion angle greater than 30° via a far-side lunar flyby without impacting the Moon, the burn performed here near lunar closest approach allows for safe passage around the Moon to these larger insertion angles. The PLF burn is retrograde for all cases, slowing the spacecraft down and enabling easier access to the DRO. The trajectories that enter the DRO between insertion angles of -30° and 30° perform the PLF after lunar closest approach, while all other trajectories have a PLF that occurs before lunar closest approach.
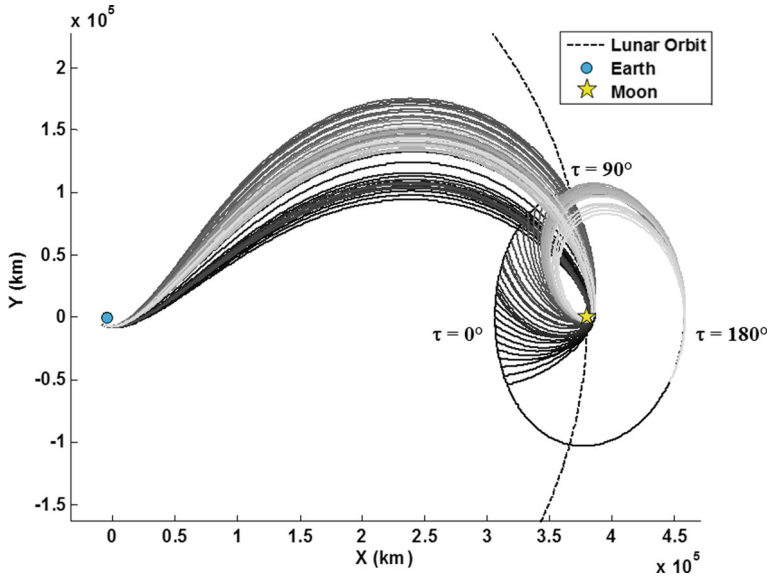
Fig. 10 Powered Lunar Flybys for τ Insertion Angles of -30° to 210°

Examination of the trajectories en-route to the PLF reveals that this is not a continuous family of trajectories like the direct transfers. This difference is likely because 1) the transfer duration is permitted to vary and 2) the transfer duration has been set to be no greater than 13 days. As will be seen later, this maximum transfer duration constraint is a primary factor in limiting the efficiency of the PLFs that enter the DRO between 170° and 210°.

Intermediate Options

While exploring the trade space, an intermediate set of PLFs was discovered. These trajectories perform a burn far away from lunar closest approach, with much of the Δv occurring at the flyby and very little occurring at DRO insertion. Figure 11 illustrates these "flybys," which in this plot occur between insertion angles of 290° and 345°. These transfers are more efficient in terms of Δv for these insertion angles compared to the PLFs depicted in Fig. 10, but they are really an indication that a direct transfer to the most efficient insertion angle of 180° is a better choice. Without the constraint to insert at an angle between approximately 290° and 345°, the optimizer would eliminate the PLF burn and instead insert at 180°, moving the burn location from the space in between the Moon and the DRO to the DRO itself. However, with the DRO insertion angles constrained, the optimizer uses large PLF burns, far from the Moon and at approximately 180°, to enable asymptotic approaches to DRO insertions with effectively 0 m/s Δv.

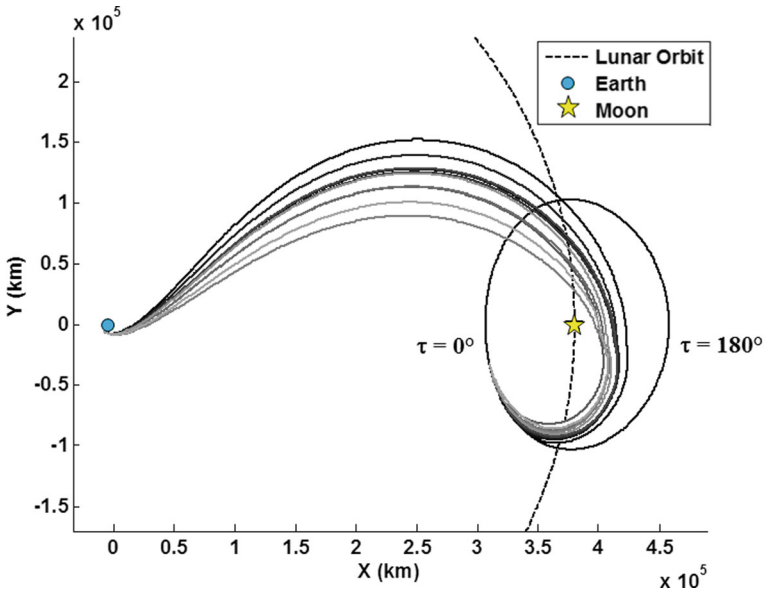**Fig. 11** Intermediate Options for Far-Side Powered Lunar Flybys

Delta-V Comparison

Figure 12 shows the Δv comparison between the direct transfers and all PLF trajectories found. The direct transfers shown are the Δv values from the right half of Fig. 8. The "regular" PLFs (from Fig. 10) are shown in circles and the intermediate
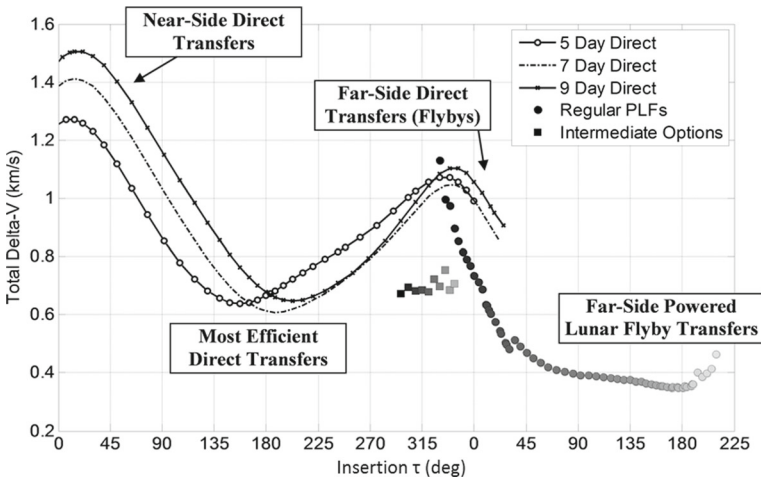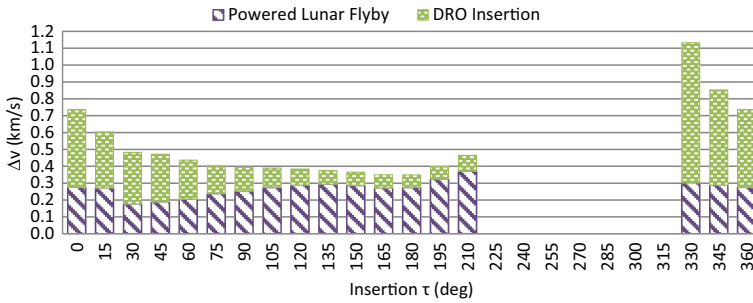

Fig. 12 Delta-V Comparison Between Far-Side Direct Transfers, Regular Powered Lunar Flybys, and Intermediate Options for Far-Side Powered Lunar Flybys

Fig. 13 Breakdown of Δv Between PLF Burn and DRO Insertion for Select Powered Lunar Flybys

PLF options (from Fig. 11) are shown in squares, both with color schemes that match Fig. 10 and Fig. 11.

The PLFs provide significant Δv savings compared to the most efficient direct transfers (∼180°) when entering the DRO between insertion angles of 15° to 210°. This is expected since, again, performing a burn close to perilune while the spacecraft is at a high velocity allows for a more efficient use of propellant and overall less Δv than the direct-transfer options. The larger required Δv for the regular PLFs between insertion angles of -30° and 15° is due to a higher altitude when passing by the Moon, causing a less efficient burn. At this point, a direct transfer that flies by the far side of the Moon and does not perform a burn near closest approach would be a better option.

At approximately 30°, a discontinuity in the PLFs occurs. The reason for this will be more apparent in the following figures, specifically Fig. 15, which shows the altitude of closest approach for the PLF trajectories.

In addition, Fig. 13 compares the Δv contributions of the PLF burn and DRO insertion for the regular class of PLF trajectories (note a subset of the trajectories are shown to more clearly represent the data). For the most efficient PLFs, occurring around 150° to 190°, a large fraction of the Δv occurs at the PLF itself, with very little Δv at the DRO insertion required afterward. Although not computed in the CRTBP, the PLFs that are missing between insertion angles of 210° and 330° are actually achievable via near-side powered lunar flybys. In addition, the Δv can be reduced for PLFs between 330° and 360° if near-side flybys are utilized instead. Examples of these types of transfers will be seen in the full-ephemeris section.

It should be noted that for all PLF trajectories found, the minimum time between the PLF burn and the DRO insertion burn is 1.2 days, satisfying the consideration that there should be at least one day between events for navigation purposes.

Transfer Duration

Figure 14 shows the transfer duration for each PLF option. The duration is shorter for the larger Δv trajectories and longer transfer durations are required for increasing τ insertion angles. At an insertion angle of approximately 170°, the trajectories begin to push up against the 13-day limitation, indicating a need for more time to reach the
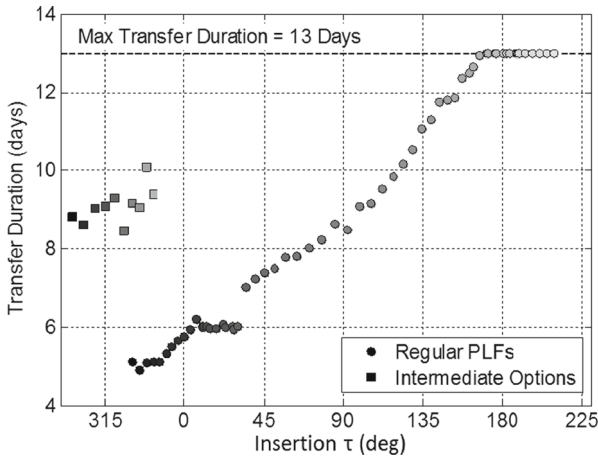
Fig. 14 Transfer Duration for Powered Lunar Flybys

DRO in order to maintain the most efficient use of Δv. This contributes to the upward trend in Δv for PLF trajectories from 170° forward seen in Fig. 12.

Altitude of Closest Approach

Figure 15 shows the altitude of closest approach for each of the regular PLF trajectories. The increase in required Δv seen in Fig. 12 as the insertion angle decreases from 15° toward -30° is caused by the corresponding increase in altitude seen here; the trajectories become less efficient by performing a burn further away from the Moon. This figure verifies that no trajectories pass below 100 km from the surface of the Moon.
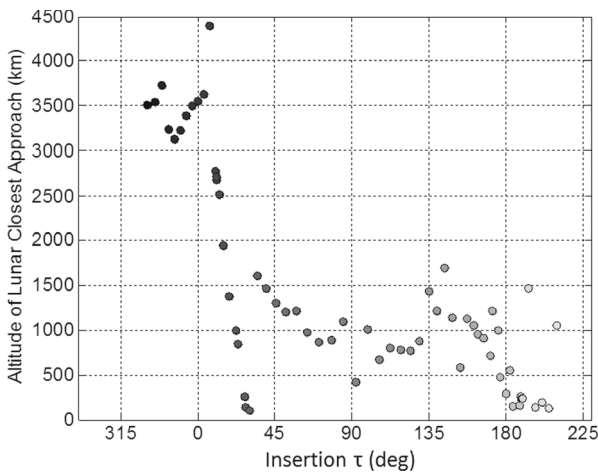
Fig. 15 Altitude of Closest Approach for Powered Lunar Flybys

Figure 15 also illustrates the source of the small discontinuities observed in previous figures. The strategy for building a trajectory at a particular insertion angle uses the previously computed trajectory at the neighboring τ value as an initial guess. As the optimizer builds trajectories from 0° toward 30°, the spacecraft flies closer and closer to the Moon. At around 30°, the optimizer hits the constraint that the trajectories must not get closer than 100 km to the surface of the Moon. This causes the jump in altitude and subsequent discontinuous behavior seen in the figures. The optimization may become more stable by simply constraining all trajectories past 30° to perform the PLF at a fixed altitude of 100 km. Nevertheless, the Δv is smaller than it was for the direct transfers from 15° forward since the trajectories still fly near the lunar surface.

Special Case: Minimum Delta-V PLF

Figure 16 depicts the minimum Δv PLF transfer from Fig. 10. It also includes a zoomed-in view of the PLF, indicating the radius of the Moon as well as the location of the PLF. The plot shows that the burn is performed before perilune, slowing the spacecraft down so that it is able to access the DRO at a larger insertion angle.

Table 3 lists various parameters for the minimum Δv trajectory seen in Fig. 16. The insertion angle is 177°. The total transfer duration is at the maximum allowed value of 13 days, with approximately twice as much time spent travelling between the PLF burn and the DRO insertion as the time spent between Earth departure and the PLF burn, indicating how the spacecraft is slowed down in order to more efficiently reach the DRO. The altitude of closest approach is 474.0 km.

The PLF burn accounts for approximately 80% of the total Δv, which serves to emphasize the potential benefit of the PLF for trajectories to DROs. The burn at the PLF is retrograde and nearly tangential, with an angle of approximately 179° between the incoming velocity vector and the Δv vector (180° indicating a perfectly retrograde burn).
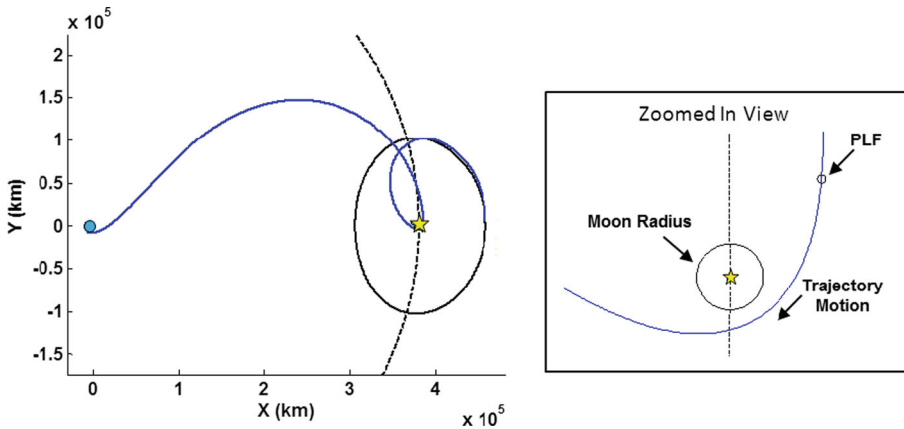
Fig. 16 Minimum Δv Powered Lunar Flyby

Table 3 Minimum Δv Powered Lunar Flyby Parameters

Parameter	Value
Tau Insertion Angle	177°
Time between Earth and PLF	4.5 days
Time between PLF and DRO	8.5 days
Total Transfer Duration	13.0 days
Altitude of Lunar Closest Approach	474.0 km
Δv at PLF	272 m/s
Direction of PLF	Retrograde Burn (179° between incoming velocity vector and Δv vector)
Δv at DRO	76 m/s
Total Δv	348 m/s

Full-ephemeris Powered Lunar Flybys

Now that the main features of transfers to DROs have been identified, it is important to examine similar trajectories produced in a high-fidelity model of the solar system. Trajectories have been generated with the same characteristics as those presented earlier, but now they have been built in a higher-fidelity force model, including the gravitational attraction of all of the planets, the Moon, and the Sun, using Jet Propulsion Laboratory (JPL) planetary ephemerides (DE405). Although the Sun's gravitation is included in the analysis, the effect of its position relative to the Earth-Moon system is negligible over the course of only 13 days spent within the Earth's sphere of influence.

For each trajectory, the LEO parking orbit is now inclined by 28.5° relative to the Earth's equator, and the Moon's orbit is inclined relative to the ecliptic according to the JPL ephemeris. The higher-fidelity analysis has used TOSOCS (Trajectory Optimization with Sparse Optimal Control Software) as the optimizer. TOSOCS is a 3 degree-of-freedom, open-loop trajectory design and optimization tool. It is FORTRAN code, developed internally at Lockheed Martin and built around the commercial-off-the-shelf optimization engine SOCS [13].

TOSOCS trajectories are divided into *phases*, where a phase may be a coast arc, an impulsive maneuver, or a finite burn. For this problem, the transfer consists of the translunar injection, the spacecraft separation from the upper state, the perilune burn, and the insertion burn, with coasts separating each maneuver. Also, two phases define the target DRO for the trajectory, which eliminates the need to reference an external DRO ephemeris. This internal calculation of the DRO allows TOSOCS to optimize the DRO geometry concurrently with the spacecraft Δv to reach a specified insertion point on the 2:1 resonant DRO. In addition, while the CRTBP PLF simulations constrain the trajectories to only fly by the far side of the Moon, TOSOCS can choose either a near-side or far-side flyby depending on which is the most optimal transfer.
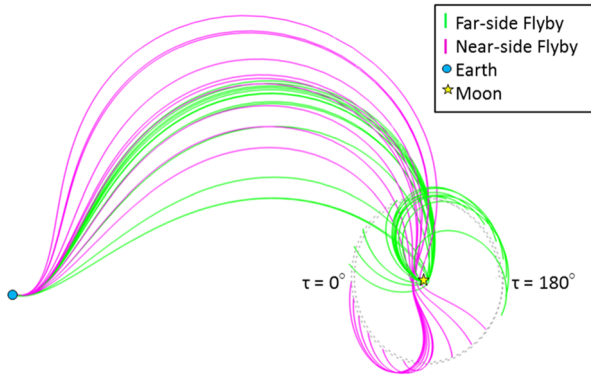
Fig. 17 Trajectories for 0° Lunar True Anomaly

High-fidelity PLF transfers in TOSOCS are constructed for τ insertion values between 0° and 360° at 15° increments (referred to as a τ "sweep"). In order to analyze the variation introduced by the Moon's elliptical orbit around the Earth, one τ sweep permits the PLF to occur at any angle of the Moon in its orbit around the Earth (the lunar true anomaly, or LTA). Four additional sweeps constrain the PLF to occur when the Moon is at an LTA of 0° (Fig. 17), 90°, 180° (Fig. 18), and 270° (the 90° and 270° cases are similar to 0° and 180°, and images are omitted for brevity).

Similar constraints have been imposed for these trajectories as for the CRTBP trajectories. The transfers may take no longer than 13 days from LEO through DRO insertion. The PLF may only occur at altitudes of 100 km or above, with the Δv in any direction (including out of plane), and cannot cause the transfer to drop below 100 km in altitude at any time. The optimal PLF burns have been observed to be primarily in-plane and retrograde, similar to results found using the CRTBP. Note that the region from 0° to about 210° in each of the following figures is comparable to
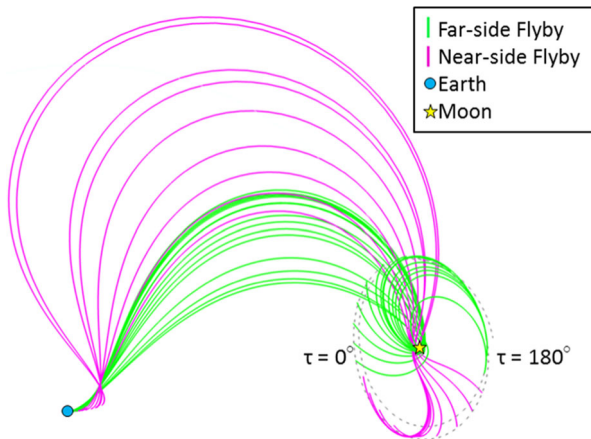
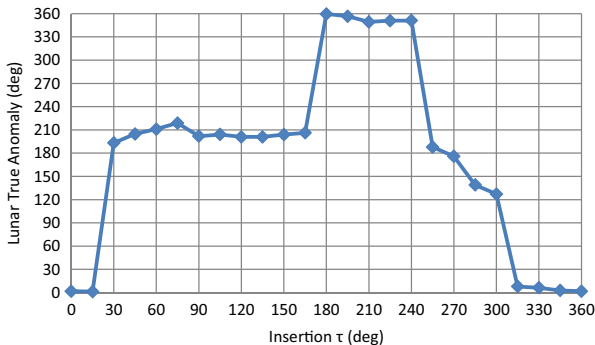**Fig. 18** Trajectories for 180° Lunar True Anomaly
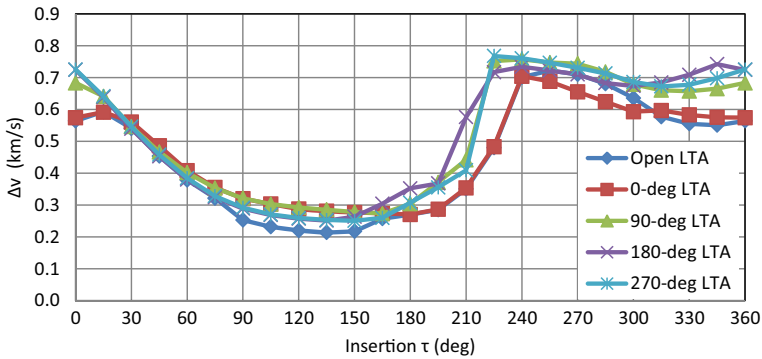
Fig. 19 DRO Insertion τ Versus Spacecraft Δv

the CRTBP PLF results, since these correspond to far-side powered lunar flybys. In addition, the trajectories found in the CRTBP from 330° to 360°, which are far-side flybys, are actually not as efficient as the near-side flybys found by TOSOCS.

The DRO insertion angle τ versus spacecraft Δv curves appear in Fig. 19. General trends include lower Δv in the region around 135° and peak Δv values near 255°. The greatest variability between the LTA cases exists between about 210° and 360°.

The trajectories that fall into the traditional far-side flyby category and circle around the Moon resemble the CRTBP results in Fig. 10, while those that complete near-side flybys are similar in appearance to the near-side direct trajectories in Fig. 4, but the addition of the PLF results in much lower Δv, as was seen in the CRTBP results.

Figure 20 provides insight for the results when the LTA is unconstrained, tracking the LTA chosen by TOSOCS at each τ. For the range of τ values between 90° and 150°, for example, the optimum LTA falls at roughly 210°. In Fig. 19, the "Open LTA" case indeed does not consistently fall directly on any of the specific LTA cases, but LTAs of 180° and 270°, those options closest to 210°, have the lowest Δv. Similarly, Fig. 20 illustrates that TOSOCS optimizes the LTA to be approximately 360°

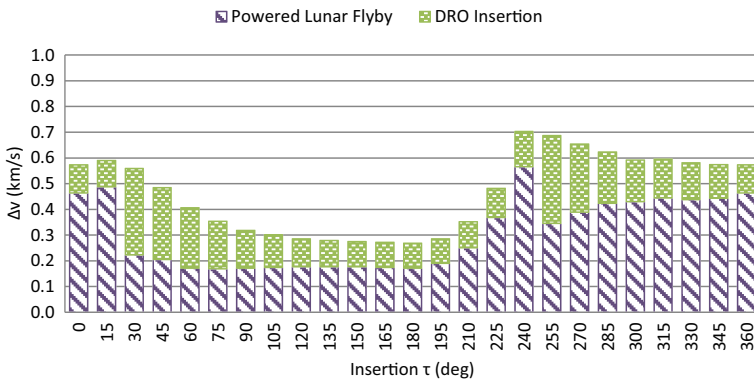**Fig. 20** DRO Insertion τ Versus Lunar True Anomaly for Unconstrained Lunar True Anomaly (at Flyby)
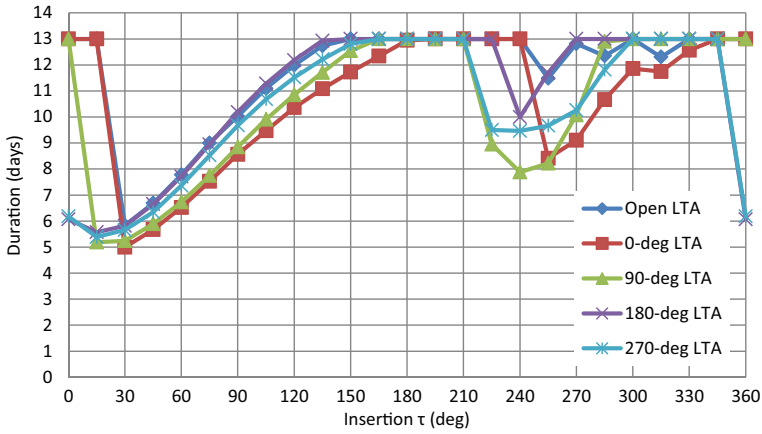
**Fig. 21** DRO Insertion τ Versus Trajectory Duration

when arriving at the DRO at τ values in the range of 180° to 240°, and Fig. 19 reveals that the curves for "Open LTA" and "0-deg LTA" line up almost exactly in this region of τ.

Figure 21 shows the duration of each trajectory. It is clear when the maximum duration constraint is active and the duration consistently reaches the upper bound of 13 days. Note that the 180° cases (corresponding to the Moon at its largest displacement from the Earth) hit the 13-day limit 12 times, since it takes longer for the spacecraft to reach the Moon when it is at apogee. The 0° cases (corresponding to the Moon at its smallest displacement from the Earth) reach the limit only 8 times.

In addition, the drop in duration around 240° is due to this duration constraint. Here, the spacecraft is unable to perform a traditional PLF burn and insert into the DRO within 13 days for τ values between about 180° and 360°. In order to reach τ values around 180° to 225°, the spacecraft trajectory curves far from the Earth-Moon line before the near-side flyby, resulting in better alignment to reach these

Fig. 22 Powered Lunar Flyby and DRO Insertion Δv Values for 0° Lunar True Anomaly
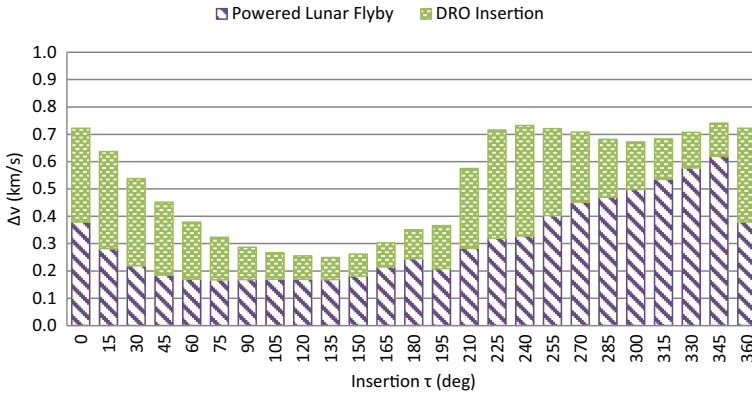
Fig. 23 Powered Lunar Flyby and DRO Insertion Δv Values for 180° Lunar True Anomaly

insertion points. However, for τ values around 240° to 270°, a more direct, shorter, near-side flyby allows insertion into the DRO.

Figures 22 and 23 show the Δv breakdown for the 0° and 180° LTA cases, respectively. The spacecraft Δv consists of the PLF and DRO insertion burns. The different LTA cases exhibit similar behavior, with the PLF dominating the total Δv in certain regions of insertion τ (approximately 90° to 195° and 270° to 360°; the regions of the smooth, overlapping trajectories in Fig. 17 and Fig. 18 where the spacecraft inserts into the DRO almost asymptotically) and the DRO insertion in others (about 15° to 75° and 210° to 255°, where the angle between the incoming trajectory and the DRO is larger). Again, the results seen here between 0° and 210° are comparable to the CRTBP PLF results seen in Fig. 13.

Conclusion

Several trajectory options exist for most DRO insertion τ angles, providing flexibility to mission planners for designing the trajectories for initiatives like ARM. Direct transfers of various durations can insert a vehicle into any part of the DRO if simplicity is a desirable mission feature, but the addition of a PLF burn reduces Δv for most cases. Modeling in both the CRTBP and real ephemeris addresses the additional complexity of missions utilizing PLFs, which may be far-side burns (CRTBP and real ephemeris) or near-side burns (real ephemeris). Navigation requirements may also affect the choice of a trajectory.

The 5-, 7-, and 9-day direct transfers can access the 2:1 DRO at all insertion angles, with some insertion angles supporting two types of trajectories. In the case where two types existed, the far-side lunar flybys achieve lower Δv than the near-side options. However, many of the flyby trajectories at low radii of

closest approach have less than one day between closest approach and DRO insertion, which is not ideal for navigation purposes. It is important to note, though, that the only reason to utilize one of these more expensive flyby trajectories, as opposed to the more efficient minimum Δv trajectories to 180°, is if the spacecraft is required to access the DRO at a particular insertion angle at a particular time.

Direct transfer trajectories that insert into the DRO at approximately 180° without using a lunar flyby are the most efficient for all three transfer durations. Furthermore, trajectories that pass by the near side of the Moon are most efficient for the 5-day duration, and those passing by the far side tend to be most efficient for the 7-day transfers. Depending on lighting and communications requirements for rendezvous missions between, for instance, the spacecraft and the asteroid, there are clearly many options and many tradeoffs to be considered when designing a direct transfer mission to a DRO.

The PLFs that pass by the far side of the Moon offer significant Δv savings of 300 m/s, on average, compared to the most efficient direct transfer trajectories. They also enable access via a far-side flyby to more extreme insertion angles than the direct transfer far-side flybys could reach, an effect of the retrograde anti-velocity burn performed near lunar closest approach. In addition, trajectories that pass closer to the Moon are often more efficient in terms of Δv. In both the CRTBP and real-ephemeris trajectories, the PLF is actually the dominant burn for about half of the cases of insertion angles.

In the real ephemeris, the trajectories that fall into the far-side category have τ values of about 0° to 210°, reminiscent of the CRTBP results, with the remainder of the trajectories falling in the near-side category. The switch from one family to another seems to occur when the trajectory runs into the duration constraint of 13 days and takes the shorter, near-side approach to reach the insertion τ. However, between the two families of trajectories, each insertion τ is accessible in 13 days or less and at any of the four main LTAs. Generally, the similar behavior of the CRTPB trajectories and those calculated using real ephemeris emphasize the many feasible options for transfers to 2:1 resonant lunar DROs. Finally, all PLF trajectories presented satisfy the need for more than one day between the PLF burn and DRO insertion burn.

Further work can be done to create additional trajectories that access DROs of different lunar resonances such as 3:1 and 4:1. There are also DROs that exist in all three dimensions, and performing an analysis on direct transfers and PLFs to these three-dimensional DROs using the full ephemeris instead of just the Circular Restricted Three-Body Problem would provide insight into more realistic trajectories for the spacecraft.

References

1. NASA: Asteroid Redirect Mission Reference Concept URL. accessed January, 2014. http://www.nasa.gov/pdf/756122main_AsteroidRedirectMissionReferenceConceptDescription.pdf

2. Strange, Nathan, Damon, Landau, Timothy McElrath, et al.: Overview of Mission Design for NASA Asteroid Redirect Robotic Mission Concept 33rd International Electric Propulsion Conference Washington, D.C. 6–10 Oct 2013

3. Brophy, John, Culick, F.red., et al.: Asteroid Retrieval Feasibility Study Keck Institute for Space Studies, California Institute of Technology, Jet Propulsion Laboratory, Pasadena, California 2 Apr 2012

4. Bezrouk, C., Parker, J.: Ballistic Capture into Distant Retrograde Orbits from Interplanetary Space," Proceedings of the AAS/AIAA Space Flight Mechanics Meeting, Paper AAS 15-302, Williamsburg, Virginia 11–15 January 2015

5. Szebehely, V.: Theory of Orbits:The Restricted Problem of Three Bodies. Academic Press, New York (1967). Print

6. Parker, J.S., Anderson, R.L.: Low-Energy Lunar Trajectory Design, DESCANSO Deep Space Communication and Navigation Series. Vol. 12. Pasadena, California: Jet Propulsion Laboratory, California Institute of Technology (2013). http://descanso.jpl.nasa.gov/Monograph/mono.cfm

7. Strömgren, E.: Connaissance actuelle des Orbites Dans le Problème des Trios Corps," Copenhagen Observatory Publications, 100. Also Bull. Astro. **9**(87), 1935 (1935)

8. Hénon, M.: Exploration numérique du problème des Trois Corps, (I), Masses Egales,Orbites Périodiques. Ann. Astrophys. **28**(3), 499–511 (1965)

9. Hénon, M.: Numerical exploration of the restricted problem. V., Hill's Case: Periodic Orbits and Their Stability. Astron.& Astrophys. **1**, 223–238 (1969)

10. Broucke, R.A.: Periodic Orbits in the Restricted Three-Body Problem with Earth-Moon Masses, 32-1168, Jet Propulsion Laboratory, California Institute of Technology. Pasadena, California (1968)

11. Lam, T., Whiffen, G.J.: Exploration of Distant Retrograde Orbits Around Europa, Paper AAS 05-110,15[th] AAS/AIAA Space Flight Mechanics Conference, Copper Mountain, Colorado 23-27 January (2005)

12. Howard, W., Louis, T.: Advanced Mathematics and Mechanics Applications Using MATLAB CRC Press, 2nd ed (1997)

13. SOCS User's Guide Release 7.1. Boeing: http://www.boeingtravel.com/assets/pdf/phantom/socs/docs/SOCS_Users_Guide.pdf